

TU-1291
KEK-QUP-2025-0028

High Frequency Spectrum of Primordial Gravitational Waves

Kamil Mudrunka^(a) and Kazunori Nakayama^(a,b)

^(a)*Department of Physics, Tohoku University, Sendai 980-8578, Japan*

^(b)*International Center for Quantum-field Measurement Systems for Studies of the Universe and Particles (QUP), KEK, 1-1 Oho, Tsukuba, Ibaraki 305-0801, Japan*

Abstract

During inflation gravitational waves are produced in the superhorizon regime, which form stochastic background in the present universe with very wide range of frequencies. Higher frequency gravitational waves never experience superhorizon regime, but they are also amplified after inflation due to the inflaton oscillation. Taking account of the inflaton dynamics after inflation, the spectrum of primordial gravitational waves may extend to much higher frequencies than previously thought. In this paper we calculate the spectrum of high frequency gravitational waves produced during and after inflation in detail, in particular focusing on the connection between the low and high frequency regime, and show that the detailed spectrum can distinguish inflation models.

Contents

1	Introduction	1
2	Quantum production of gravitational waves	3
2.1	Formalism	3
2.2	Gravitational wave spectrum	6
2.3	Analytic estimation	6
3	Gravitational wave spectrum in concrete models	10
3.1	Chaotic inflation	10
3.2	Starobinsky inflation	11
3.3	New inflation	12
3.4	Attractor inflation	14
4	Conclusions and discussion	16
A	Convention	17

1 Introduction

During inflation [1–6], scalar and tensor perturbations are stretched and exit the horizon. Superhorizon scalar perturbations generated during inflation are considered to be the origin of the structure of the universe. On the other hand, superhorizon tensor perturbations form the so-called primordial gravitational waves (GWs), which result in the stochastic GW background in the present universe with various frequencies, ranging from cosmological scales to terrestrial scales [7–13]. If primordial GWs will be detected in future, it provides us with the information about the inflation energy scale.

Not only the inflation energy scale, but also the information about thermal history of the universe after inflation is contained in the primordial GW spectrum [14–28]. If the equation of state parameter of the universe is w when a superhorizon GW mode with comoving wavenumber k re-enters the horizon, the resulting GW spectrum scales as $\Omega_{\text{GW}} \propto k^{2(3w-1)/(1+3w)}$ [15, 17, 19] (see Eq. (30)). Therefore, the spectral shape of primordial GWs directly tells us thermal history of the universe. Note that these arguments apply to the GW modes that once experienced superhorizon regime during inflation, i.e., $k \lesssim a_e H_e \equiv k_1$ where a_e and H_e are the scale factor and the Hubble scale at the end of inflation, respectively. A schematic picture of the GW spectrum for $w = 0$ is shown in Fig. 1: the $k < k_1$ part corresponds to the modes that experienced superhorizon regime during inflation. The flat part in the region $k_{\text{eq}} < k < k_R$, where k_{eq} and k_R are the comoving Hubble scale at the matter-radiation equality and the end of reheating, corresponds to the mode that re-enter the horizon during radiation-dominated era.

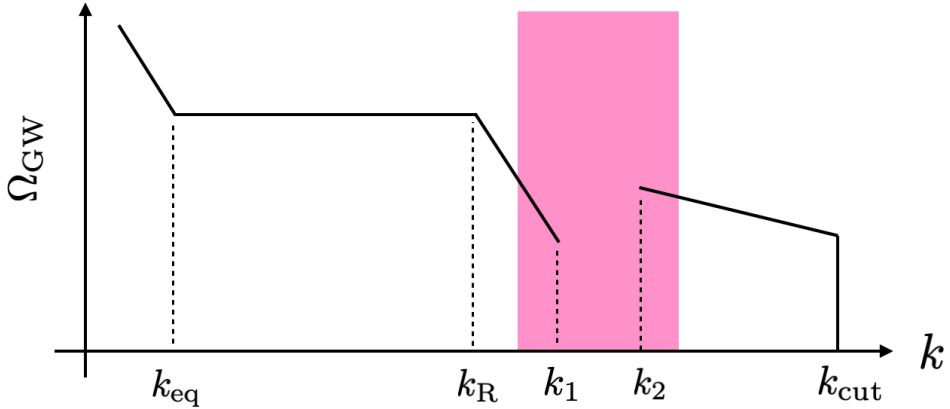


Figure 1: Schematic picture of the primordial GW spectrum for the case of $w = 0$. Several characteristic comoving wavenumber are plotted: k_{eq} and k_{R} are the comoving Hubble scale at the matter-radiation equality and the end of reheating, respectively, and k_{cut} is the comoving inflaton mass scale at the end of reheating. For k_1 and k_2 , see text. Our main focus is the behavior around the red shaded region.

Recently it has been pointed out in Refs. [29–31] that even higher frequency modes $k \gg k_1$ may be excited due to the post-inflationary inflaton dynamics. This is because the inflaton exhibits coherent oscillation and there appears an inflaton mass scale m_ϕ , which is typically (much) larger than the Hubble scale, after inflation ends. This is nothing but particle production due to the rapidly oscillating background through the gravitational interaction [32–36], and can intuitively be regarded as inflaton annihilation to the graviton pair [29–31, 37–39]. This may result in a high frequency tail in the GW spectrum that extends to $k \gg k_1$.¹ If the inflaton oscillation proceeds through quadratic inflaton potential, i.e. $w = 0$, such high frequency tail scales as $k^{-1/2}$ for $k \gg k_2 \equiv a_{\text{e}} m_\phi$ [29, 31]. This contribution is schematically shown in Fig. 1: the high frequency spectrum extends to $k > k_2$ and there is eventually a cutoff at $k = k_{\text{cut}}$, the comoving inflaton mass scale at the end of reheating.²

Therefore, the primordial GW spectrum for $k \lesssim k_1$ and $k \gtrsim k_2$ are relatively well understood. However, depending on inflation models, there is large hierarchy between k_1 and k_2 and the spectrum at intermediate frequency range $k_1 \lesssim k \lesssim k_2$ has not been explored. The purpose of this paper is to precisely calculate the GW spectrum across the intermediate frequency range, as shown by the red shaded region in Fig. 1. Technically, the GW spectrum at low frequency limit is easily calculated in a classical way, while the Bogoliubov method is

¹In this paper we also call such high frequency GWs “primordial GWs”. It is partly because the production of both low and high frequency modes are governed by exactly the same GW equation of motion under the homogeneous inflaton dynamics. Thus they are indistinguishable in rigorous sense, and actually the transition from the low to high frequency regime is smooth.

²For $w > 1/3$, the contribution from inflaton oscillation extends toward *lower* frequency [37], as we will explain in Sec. 2.

efficient for calculating the high frequency limit. The intermediate frequency range requires careful treatment, and we will develop methods that can be applied to such a frequency range.

This paper is organized as follows. In Sec. 2 we give a formalism to calculate the primordial GW spectrum. In Sec. 3 we calculate the GW spectrum for several concrete inflation models. Sec. 4 is devoted to conclusions and discussion.

2 Quantum production of gravitational waves

2.1 Formalism

The GW or graviton can be identified as the tensor perturbation of the metric. We define the tensor perturbation h_{ij} around the Friedmann-Robertson-Walker metric as (see App. A for our convention)

$$ds^2 = -dt^2 + a^2(t)(\delta_{ij} + h_{ij}(t, \vec{x}))dx^i dx^j, \quad (1)$$

where $a(t)$ is the scale factor. Let us Fourier expand h_{ij} in terms of the creation-annihilation operators as

$$h_{ij}(t, \vec{x}) = \sum_{\lambda=+,\times} \int \frac{d^3k}{(2\pi)^3} \left[a_{k,\lambda} h_{k,\lambda}(t) + a_{-k,\lambda}^\dagger h_{k,\lambda}^*(t) \right] e^{i\vec{k}\cdot\vec{x}} e_{ij}^\lambda, \quad (2)$$

where the polarization tensor satisfies $e_{ij}^\lambda e_{ij}^{*\lambda'} = \delta_{\lambda\lambda'}$. The creation-annihilation operators satisfy the commutation relation

$$[a_{k,\lambda}, a_{k',\lambda'}^\dagger] = (2\pi)^3 \delta(\vec{k} - \vec{k}') \delta_{\lambda\lambda'}. \quad (3)$$

We assume the standard Einstein-Hilbert action for a gravity sector. Then the equation of motion of the graviton is

$$\ddot{h}_{k,\lambda} + 3H\dot{h}_{k,\lambda} + \left(\frac{k}{a}\right)^2 h_{k,\lambda} = 0, \quad (4)$$

where the dot denotes the derivative with respect to time t and $H = \dot{a}/a$ denotes the Hubble parameter. By defining $\tilde{h}_{k,\lambda} \equiv ah_{k,\lambda}$, the equation of motion is also written as

$$\tilde{h}_{k,\lambda}'' + \omega_k^2 \tilde{h}_{k,\lambda} = 0, \quad \omega_k^2 = k^2 - \frac{a''}{a}, \quad (5)$$

where the prime denotes the derivative with respect to the conformal time $\tau = \int \frac{dt}{a}$. The initial condition is given in the high frequency limit $k \gg aH$ as

$$\tilde{h}_{k,\lambda}(\tau) = \frac{1}{\sqrt{2k}} e^{-ik\tau}. \quad (6)$$

In the superhorizon limit $k \ll aH$ during inflation, the asymptotic solution is

$$\tilde{h}_{k,\lambda}(\tau) = i \frac{aH_{\text{inf}}}{\sqrt{2}k^{3/2}}, \quad (7)$$

where H_{inf} denotes the Hubble scale during inflation.³

Semi-classical method

A straightforward method to evaluate the produced GW energy density is just to solve the equation of motion (4) with initial condition (6), under the background inflaton motion:

$$\ddot{\phi} + 3H\dot{\phi} + \frac{\partial V}{\partial \phi} = 0, \quad (8)$$

$$3H^2 M_{\text{Pl}}^2 = \frac{\dot{\phi}^2}{2} + V, \quad (9)$$

where ϕ is the inflaton and V is its scalar potential. Concrete inflation models will be listed in the following sections. In this formalism, the Hubble parameter H oscillates after inflation ends and it results in the graviton production [29, 31]. The resulting GW energy density is given by

$$a^4(\tau)\rho_h(\tau) = 2 \int \frac{d^3k}{(2\pi)^3} \frac{1}{2} \left[\left| \tilde{h}'_{k,\lambda}(\tau) \right|^2 + k^2 \left| \tilde{h}_{k,\lambda}(\tau) \right|^2 - k \right] \quad (10)$$

$$\equiv \int d\ln k a^4(\tau)\rho_h(k, \tau) \quad (11)$$

where

$$a^4(\tau)\rho_h(k, \tau) = \frac{k^3}{2\pi^2} \left[\left| \tilde{h}'_{k,\lambda}(\tau) \right|^2 + k^2 \left| \tilde{h}_{k,\lambda}(\tau) \right|^2 - k \right]. \quad (12)$$

Here the divergent zero-point energy is subtracted. We call this the ‘‘semi-classical method’’, since we just need to solve the equation of motion (4) along with (8) and (9) to derive the resulting GW energy density, although the actual production process is purely quantum since we start from the zero-point fluctuation (6) of the graviton field as the initial condition.

In principle this method works for arbitrary low and high graviton momenta, but for practical numerical calculation this method becomes more and more inefficient for high frequency limit $k \gg aH$ since we need extremely high precision to properly subtract the divergent part. In the high frequency limit, the following Bogoliubov method is much more efficient.

³The Hubble scale slowly changes during inflation. In this paper we are mostly interested in the Hubble parameter around the end of inflation, which we denote by H_e hereafter.

Bogoliubov method

In the Bogoliubov method, we further decompose $\tilde{h}_{k,\lambda}(\tau)$ as

$$\tilde{h}_{k,\lambda}(\tau) = \alpha_k(\tau)v_k(\tau) + \beta_k(\tau)v_k^*(\tau), \quad v_k(\tau) \equiv \frac{1}{\sqrt{2k}}e^{-i\Omega_k}, \quad (13)$$

where $\alpha_k(\tau)$ and $\beta_k(\tau)$ are called Bogoliubov coefficient and $\Omega_k(\tau) = \int \omega_k(\tau)d\tau$. They are chosen to satisfy the following relation:

$$\alpha'_k(\tau) = \frac{\omega'_k}{2\omega_k}\beta_k e^{2i\Omega_k}, \quad \beta'_k(\tau) = \frac{\omega'_k}{2\omega_k}\alpha_k e^{-2i\Omega_k} \quad (14)$$

The initial condition (6) is written as $\alpha_k(\tau) = 1$ and $\beta_k(\tau) = 0$ in this language. One can easily prove that the relation $|\alpha_k(\tau)|^2 - |\beta_k(\tau)|^2 = 1$ always holds. This equation is also rewritten as

$$A'_k = -i\omega_k A_k + \frac{\omega'_k}{2\omega_k} B_k, \quad B'_k = i\omega_k B_k + \frac{\omega'_k}{2\omega_k} A_k, \quad (15)$$

by defining $A_k \equiv \alpha_k e^{-i\Omega_k}$ and $B_k \equiv \beta_k e^{i\Omega_k}$. For readers' convenience, we list some useful equations to numerically evaluate this equation:

$$\frac{a''}{a} = a^2(2H^2 + \dot{H}), \quad (16)$$

$$\omega'_k = -\frac{a^3}{2\omega_k} \left(\ddot{H} + 6H\dot{H} + 4H^3 \right), \quad (17)$$

$$\dot{H} = -\frac{\dot{\phi}^2}{2M_{\text{Pl}}^2}, \quad \ddot{H} = \frac{\dot{\phi}}{M_{\text{Pl}}^2} \left(3H\dot{\phi} + \frac{\partial V}{\partial \phi} \right). \quad (18)$$

One can integrate the equation (14) or (15) along with the background evolution (8) and (9) to obtain the Bogoliubov coefficients at arbitrary later time. One should note that ω_k becomes zero at the horizon crossing and the equation (14) or (15) becomes singular. Thus the Bogoliubov method is only useful for high frequency modes that never exit the horizon.

In terms of the Bogoliubov coefficients, the renormalized graviton energy density is given by

$$a^4(\tau)\rho_h(\tau) = 2 \int \frac{d^3k}{(2\pi)^3} k |\beta_k(\tau)|^2, \quad (19)$$

and hence

$$a^4(\tau)\rho_h(k, \tau) = \frac{k^4}{\pi^2} |\beta_k(\tau)|^2. \quad (20)$$

Thus β_k counts only the physically produced particles. In this method we do not need to worry about the subtraction of the divergent part: it is already subtracted.

2.2 Gravitational wave spectrum

Once we evaluate the GW energy density by Eqs. (12) or (20) at some fixed cosmological time $t = t_c$, it is converted to the present GW density parameter $\Omega_{\text{GW}}(f)$. To do so, we need to assume background evolution of the universe.

Our basic assumption is that the inflaton oscillates around the potential minimum after inflation ends. Let us expand the inflaton field around its vacuum expectation value v as $\phi = v + \varphi$ and suppose that the potential is approximated by $V \propto \varphi^n$ near the potential minimum. The effective equation of state parameter w during the inflaton oscillation regime is given by

$$w = \frac{n-2}{n+2}, \quad (21)$$

and the inflaton energy density decreases as $\rho_\phi \propto a^{-3(1+w)} = a^{-\frac{6n}{n+2}}$. Such an inflaton oscillation regime lasts for a while, and finally the inflaton is assumed to decay and reheat the universe. After the decay, the universe enters the radiation-dominated regime. The reheating temperature is represented by T_R hereafter.

With these assumptions, the present GW density parameter is given by

$$\Omega_{\text{GW}}(f) = \frac{\rho_h(k, t_0)}{\rho_{\text{crit}}(t_0)} \quad (22)$$

$$= \Omega_r \times \frac{g_{*R}}{g_{*0}} \left(\frac{g_{*s0}}{g_{*sR}} \right)^{\frac{1}{3}} \times \left(\frac{H_R}{H_c} \right)^{\frac{2(1-3w)}{3(1+w)}} \times \frac{\rho_h(k, t_c)}{3H_c^2 M_{\text{Pl}}^2}, \quad (23)$$

where Ω_r is the radiation density parameter and the subscript 0, R and c represent the present time $t = t_0$, reheating time ($T = T_R$) and $t = t_c$, respectively.⁴ The comoving wavenumber k and the present GW frequency f is related as

$$f = \frac{k}{2\pi a_0} = \frac{k}{2\pi a_c} \times \left(\frac{g_{*s0}}{g_{*sR}} \right)^{\frac{1}{3}} \times \frac{T_0}{T_R} \times \left(\frac{H_R}{H_c} \right)^{\frac{2}{3(1+w)}}, \quad (24)$$

$$= \frac{k}{2\pi a_R} \times \left(\frac{g_{*s0}}{g_{*sR}} \right)^{\frac{1}{3}} \times \frac{T_0}{T_R}, \quad (25)$$

where T_0 is the present cosmic temperature. In the following sections, we assume $T_R = 10^{10} \text{ GeV}$ as a representative value and $g_{*R} = g_{*sR} = 106.75$.

2.3 Analytic estimation

Here we give a rough estimation of the qualitative behavior of the GW spectrum. Let us consider a typical situation shown in the left panel of Fig. 2 for $w < 1/3$ and Fig. 3 for

⁴Here $g_{*0} = 3.36$, $g_{*s0} = 3.909$ and $\Omega_r \simeq 8.5 \times 10^{-5}$ are defined as if all neutrinos were massless. If one wants to avoid the confusion, one could use $g_*(T_{\text{eq}}) = 3.36$ and $g_{*s}(T_{\text{eq}}) = 3.909$ at the matter-radiation equality instead of g_{*0} and g_{*s0} , and the photon density parameter Ω_γ by replacing $\Omega_r = (g_{*0}/2)\Omega_\gamma$.

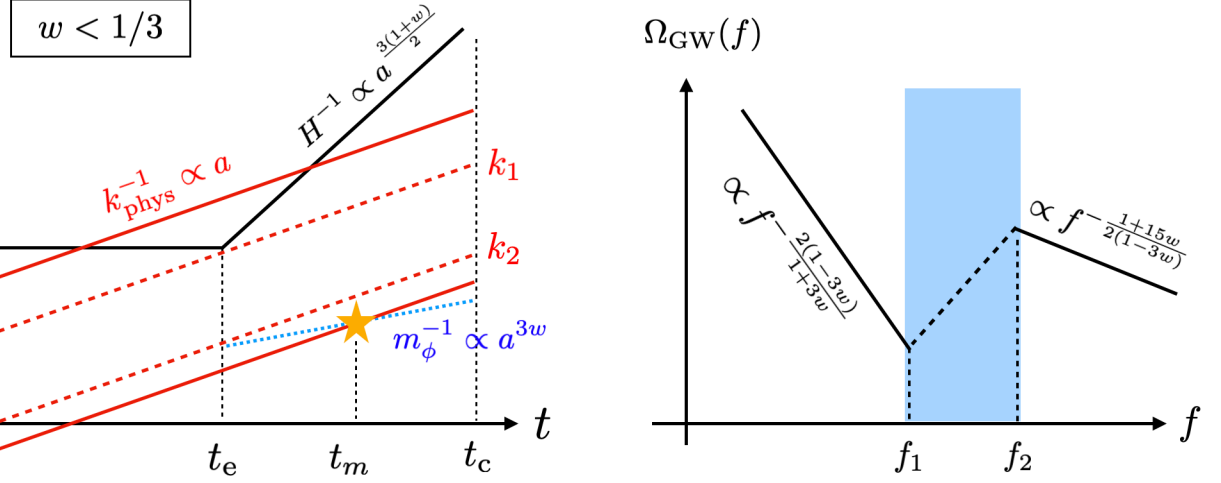


Figure 2: (Left) Time evolution of several length scales: Hubble scale H^{-1} (black line), physical GW wavelength a/k (red lines), the effective inflaton mass scale m_ϕ^{-1} (blue dashed line). The time at the end of inflation is represented by t_e and the star represents when the condition $k = am_\phi$ is satisfied for one choice of k at $t = t_m$, at which particle production happens. (Right) Expected GW spectrum as a function of (present) GW frequency f : f_1 and f_2 correspond to the comoving wavenumber k_1 and k_2 . The blue shaded region is hard to predict analytically and we need numerical simulation to derive the behavior in this region. We assumed $w < 1/3$ in this figure, where w is the equation of state parameter during the inflaton oscillation epoch.

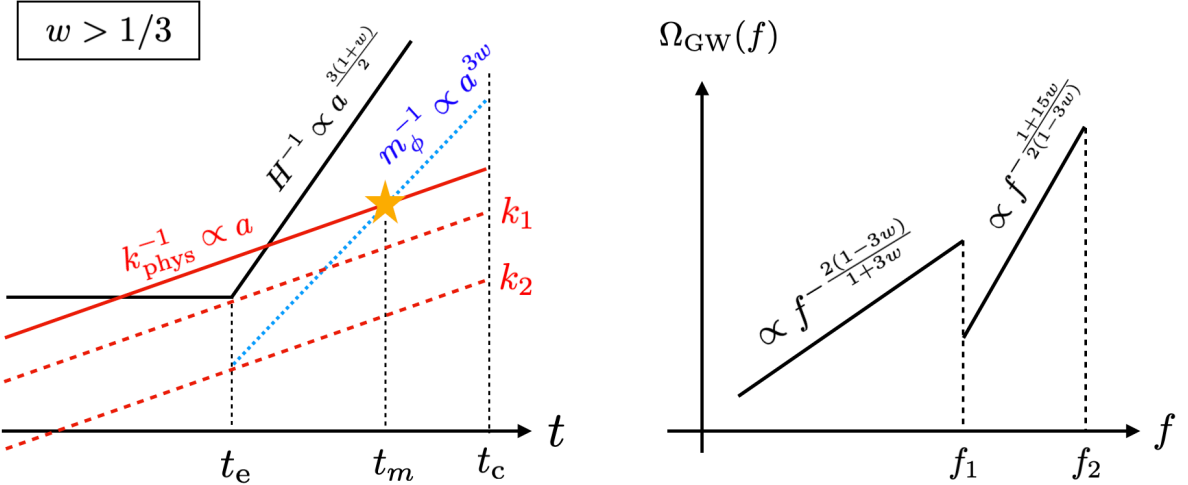


Figure 3: The same as Fig. 2, but for $w > 1/3$.

$w > 1/3$, in which the time evolution of the Hubble horizon scale and several typical physical wavelength are shown. The time at which inflation ends is denoted by t_e .

Long wavelength limit

First we focus on the GW modes that once exit the horizon during inflation, $k \ll a_e H_e$. In this case, the GW amplitude is frozen at the value $\frac{k^3 h_k^2}{2\pi^2} \sim \left(\frac{H_e}{2\pi}\right)^2$ independent of the wavenumber, as expected from (7).⁵ After it re-enters the horizon, the GW amplitude decreases as $h_k \propto a^{-1}$. Thus the GW energy density at $t = t_c$ is given by

$$\rho_h(k, t_c) \simeq \frac{k^3 h_k^2(t_c)}{2\pi^2} \left(\frac{k}{a_c}\right)^2 \simeq \left(\frac{H_e}{2\pi} \frac{a_k}{a_c}\right)^2 \left(\frac{k}{a_c}\right)^2, \quad (26)$$

where $a_k = a(t_k)$ with t_k defined by the time at the horizon re-entry: $k = a(t_k)H(t_k)$. By using

$$\frac{a_k}{a_e} = \left(\frac{a_e H_e}{k}\right)^{\frac{2}{1+3w}}, \quad (27)$$

we obtain

$$\rho_h(k, t_c) \simeq \frac{H_e^4}{4\pi^2} \left(\frac{a_e}{a_c}\right)^4 \left(\frac{a_e H_e}{k}\right)^{\frac{2(1-3w)}{1+3w}}. \quad (28)$$

This reproduces the well known result that the GW spectrum is flat for the modes that enter the horizon at the radiation-dominated era ($w = 1/3$) and the spectrum scales as k^{-2} for those which enter the horizon at the matter-dominated era ($w = 0$) [16, 17]. In terms of $\Omega_{\text{GW}}(f)$, with the use of formula (23), we obtain

$$\Omega_{\text{GW}}(f) = \Omega_r \times \frac{g_{*R}}{g_{*0}} \left(\frac{g_{*s0}}{g_{*sR}}\right)^{\frac{4}{3}} \times \frac{H_e^2}{12\pi^2 M_{\text{Pl}}^2} \left(\frac{H_R}{H_e}\right)^{\frac{2(1-3w)}{3(1+w)}} \left(\frac{a_e H_e}{k}\right)^{\frac{2(1-3w)}{1+3w}} \quad (29)$$

$$= \Omega_r \times \frac{g_{*R}}{g_{*0}} \left(\frac{g_{*s0}}{g_{*sR}}\right)^{\frac{4}{3}} \times \frac{H_e^2}{12\pi^2 M_{\text{Pl}}^2} \left(\frac{a_R H_R}{k}\right)^{\frac{2(1-3w)}{1+3w}}. \quad (30)$$

Note that the t_c dependence is gone as it should be.

Short wavelength limit

Next let us consider GWs with short wavelength limit, which never exit the horizon. As far as $k \gg aH_{\text{inf}}$, the evolution of the modes are adiabatic during inflation and no enhancement happens. However, after inflation, the inflaton coherent oscillation begins and then another mass scale, the inflaton mass m_ϕ , appears. It is sometimes much larger than the Hubble

⁵Here we neglect a small k dependence characterized by the slow-roll parameter.

scale H_{inf} . Then the GW modes enhancement happens when the condition $k/a \simeq m_\phi$ is satisfied. This is nothing but a particle production due to the oscillating field, and a simple (rough) interpretation is that the gravitons are produced by the inflaton annihilation process $\varphi\varphi \rightarrow hh$ [29, 31]. For the inflaton potential $V \sim \varphi^n$, the effective “mass” of the inflaton is given by $m_\phi \propto \varphi^{(n-2)/2} \propto a^{-3w}$ and there may also be multi inflaton annihilation processes like $\varphi \cdots \varphi \rightarrow hh$.

The effective production rate of the graviton from the inflaton is given by

$$\Gamma_{\varphi\varphi \rightarrow hh} \sim \mathcal{C} \frac{\langle \varphi^2 \rangle m_\phi^3}{M_{\text{Pl}}^4}, \quad (31)$$

where $\mathcal{C} \sim 10^{-2}$ is a numerical factor. Let us define the graviton production time t_m so that it satisfies $k \simeq a(t_m)m_\phi(t_m)$. The produced graviton energy density with the momentum k is given by

$$\rho_h(k, t_c) \sim \rho_\phi(t_m) \frac{\Gamma_{\varphi\varphi \rightarrow hh}}{H(t_m)} \left(\frac{a_m}{a_c} \right)^4 \sim \mathcal{C} m_\phi(t_m) H^3(t_m) \left(\frac{a_m}{a_c} \right)^4. \quad (32)$$

By using

$$\frac{a_m}{a_e} = \left(\frac{k}{a_e m_\phi(t_e)} \right)^{\frac{1}{1-3w}}, \quad (33)$$

we can rewrite the GW energy density as

$$\rho_h(k, t_c) \sim \mathcal{C} m_\phi(t_e) H_e^3 \left(\frac{a_e}{a_c} \right)^4 \left(\frac{a_e m_\phi(t_e)}{k} \right)^{\frac{1+15w}{2(1-3w)}}. \quad (34)$$

It reproduces the known result that the spectrum scales as $k^{-1/2}$ for constant inflaton mass ($w = 0$) [29, 31]. In terms of $\Omega_{\text{GW}}(f)$, with the use of formula (23), we obtain

$$\Omega_{\text{GW}}(f) = \Omega_r \times \frac{g_{*R}}{g_{*0}} \left(\frac{g_{*s0}}{g_{*sR}} \right)^{\frac{4}{3}} \times \frac{\mathcal{C} m_\phi(t_e) H_e}{3M_{\text{Pl}}^2} \left(\frac{H_R}{H_e} \right)^{\frac{2(1-3w)}{3(1+w)}} \left(\frac{a_e m_\phi(t_e)}{k} \right)^{\frac{1+15w}{2(1-3w)}}. \quad (35)$$

Several remarks are in order. First, the expression (34) is divergent for $w = 1/3$ (or $n = 4$). This represents the fact that $a(t)m_\phi(t) = \text{const.}$ and hence the condition $k = a(t)m_\phi(t)$ continues to be satisfied for a specific wavenumber k . Thus the (narrow) parametric resonance happens [33–36] and the present simple treatment breaks down.

Second, for $w > 1/3$ (or $n > 4$), m_ϕ redshifts faster than the physical wavenumber k/a .⁶ In this case, the GW modes that once exit the horizon during inflation can satisfy the

⁶In this case one should take account of the growth of the inflaton fluctuation due to self interactions, which eventually terminates the kination regime and w approaches to $1/3$ [40–42]. In this paper we just take the timing of the beginning of the $w = 1/3$ regime as a free parameter.

condition $k = am_\phi$ and hence are amplified after horizon re-entry (see the left panel of Fig. 3). Therefore, for these modes, we must take account of *both* the superhorizon enhancement and the particle production from the inflaton oscillation for the same GW mode, though our calculation will show that the latter effect is negligible. In short, the contribution from inflaton oscillation for $k < k_1$ is smaller than and hidden by the conventional primordial GWs generated during inflation.⁷

Third, for $w < 1/3$, the resultant GW energy density in the high-frequency limit (34) at $k = a_e m_\phi(t_e) \equiv k_2$ is larger than that of the low-frequency limit (28) at $k = a_e H_e \equiv k_1$ by a factor $m_\phi(t_e)/H_e$. Thus we have

$$\frac{\Omega_{\text{GW}}(f_2)}{\Omega_{\text{GW}}(f_1)} \sim \frac{m_\phi(t_e)}{H_e}, \quad (36)$$

which is typically (much) larger than unity (see the right panel of Fig. 2). The scaling for $k \ll k_1$ and $k \gg k_2$ are derived above, but the behavior at the intermediate region $k_1 \lesssim k \lesssim k_2$ is difficult to derive in an analytic way. In the following sections we numerically evaluate the GW spectrum across these regions for several concrete inflation models.

3 Gravitational wave spectrum in concrete models

In this section we calculate the primordial GW spectrum, especially focusing on the high frequency tail, based on the formalism developed in the previous section. We do not much care about the consistency of the scalar spectral index and the tensor-to-scalar ratio with cosmological observations [43], since it is not difficult to (slightly) modify the inflaton potential in order to make the model consistent with observations, while not affecting the dynamics around/after the end of inflation. In order to calculate $\Omega_{\text{GW}}(f)$, we will take $T_R = 10^{10} \text{ GeV}$ in this section.

3.1 Chaotic inflation

As the simplest example we start from the quadratic inflaton potential [44]

$$V = \frac{1}{2} m_\phi^2 \phi^2. \quad (37)$$

The dimensionless power spectrum of the curvature perturbation is given by [45]

$$\mathcal{P}_\zeta = \frac{N^2 m_\phi^2}{6\pi^2 M_{\text{Pl}}^2}, \quad (38)$$

with N being the e-folding number measured from the end of inflation, while the scalar spectral index n_s and tensor-to-scalar ratio r are given by [45]

$$n_s = 1 - \frac{2}{N}, \quad r = \frac{8}{N}. \quad (39)$$

⁷This point has been overlooked in Ref. [37].

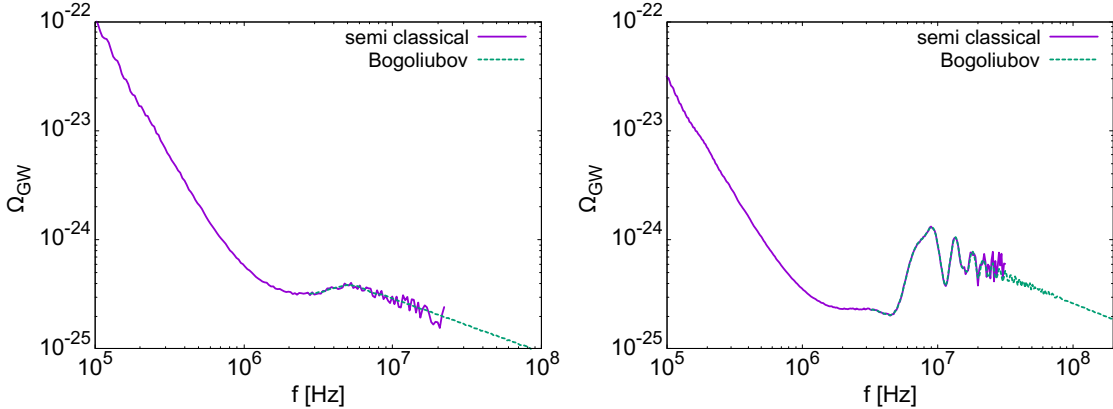


Figure 4: (Left) GW spectrum for quadratic chaotic inflation. (Right) GW spectrum for Starobinsky inflation. We have taken $T_R = 10^{10}$ GeV. Solid line is the result of semi-classical method and the dashed line is the result of Bogoliubov method. Both give consistent results in the overlapping region where the both methods are applicable. It is clearly seen that the spectrum scales as f^{-2} in the low frequency limit and $f^{-1/2}$ in the high frequency limit, as expected (see Fig. 2).

The inflaton mass is $m_\phi \sim 1.4 \times 10^{13}$ GeV to reproduce the density perturbation of the universe, $\mathcal{P}_\zeta \simeq 2.2 \times 10^{-9}$ [43].

The result of $\Omega_{\text{GW}}(f)$ is shown in the left panel of Fig. 4. In the low-frequency region we used the semi-classical method, while in the high frequency region we used the Bogoliubov method. There are overlapping regions where the both methods are useful, and we obtained consistent results. The behavior $\Omega_{\text{GW}}(f) \propto f^{-2}$ for $f < f_1$ and $\Omega_{\text{GW}}(f) \propto f^{-1/2}$ for $f > f_2$ are clearly seen, consistent with the estimation in the previous section, which is schematically shown in Fig. 2 with $w = 0$. In this model H_e and m_ϕ (hence f_1 and f_2) are the same order and the existence of the blue region in Fig. 2 is not so obvious. But still there seems to be a transition region where the spectrum shows a nontrivial behavior.⁸

3.2 Starobinsky inflation

In the Starobinsky inflation model [1], the R^2 term is introduced in the action with R being the Ricci curvature. After appropriate conformal transformation to go to the Einstein frame, a scalaron degree of freedom appears, which is identified as the inflaton. The scalar potential for the inflaton is given by

$$V = \frac{3m_\phi^2 M_{\text{Pl}}^2}{4} \left[1 - \exp \left(-\sqrt{\frac{2}{3}} \frac{\phi}{M_{\text{Pl}}} \right) \right]^2. \quad (40)$$

⁸This peculiar structure had already been seen in Ref. [31].

The dimensionless power spectrum of the curvature perturbation is given by

$$\mathcal{P}_\zeta = \frac{N^2 m_\phi^2}{24\pi^2 M_{\text{Pl}}^2}. \quad (41)$$

The inflaton mass should be $m_\phi \simeq 3 \times 10^{13}$ GeV for reproducing the cosmological observations. The scalar spectral index and tensor-to-scalar ratio are given by

$$n_s = 1 - \frac{2}{N}, \quad r = \frac{12}{N^2}. \quad (42)$$

In the minimal Starobinsky model, the reheating temperature is determined by the inflaton decay rate into the Higgs particles as (see e.g. Refs. [46, 47])

$$T_{\text{R}} \simeq 5 \times 10^9 \text{ GeV} \times |1 - 6\xi|, \quad (43)$$

where ξ denotes the nonminimal coupling between the Higgs and Ricci curvature. Thus the choice of $T_{\text{R}} = 10^{10}$ GeV is natural in this model.

The result of $\Omega_{\text{GW}}(f)$ is shown in the right panel of Fig. 4. Similar to the chaotic inflation, both the f^{-2} behavior in the low frequency limit and $f^{-1/2}$ behavior in the high frequency limit are clearly seen. An intermediate region is a bit broader and the structure is more prominent than the case of chaotic inflation.

3.3 New inflation

Next we consider new inflation model [5, 6], in which the inflaton rolls down the potential toward the symmetry breaking vacuum expectation value. In this paper we define the new inflation model by the following potential [48–54]

$$V = \Lambda^4 \left[1 - \left(\frac{\phi}{v} \right)^n \right]^2. \quad (44)$$

In this model there are two parameters, Λ and v , and hence there is a degree of freedom to choose the inflationary Hubble scale and the inflaton mass. The dimensionless power spectrum of the curvature perturbation is given by

$$\mathcal{P}_\zeta = \frac{1}{12\pi^2} \left[2n ((n-2)N)^{n-1} \right]^{\frac{2}{n-2}} \frac{\Lambda^4}{(v^n M_{\text{Pl}}^{n-4})^{\frac{2}{n-2}}}. \quad (45)$$

Scalar spectral index and tensor-to-scalar ratio is

$$n_s = 1 - \frac{2}{N} \frac{n-1}{n-2}, \quad r = \frac{16n}{N(n-2)} \left[\frac{1}{2n(n-2)N} \frac{v^2}{M_{\text{Pl}}^2} \right]^{\frac{n}{n-2}}. \quad (46)$$

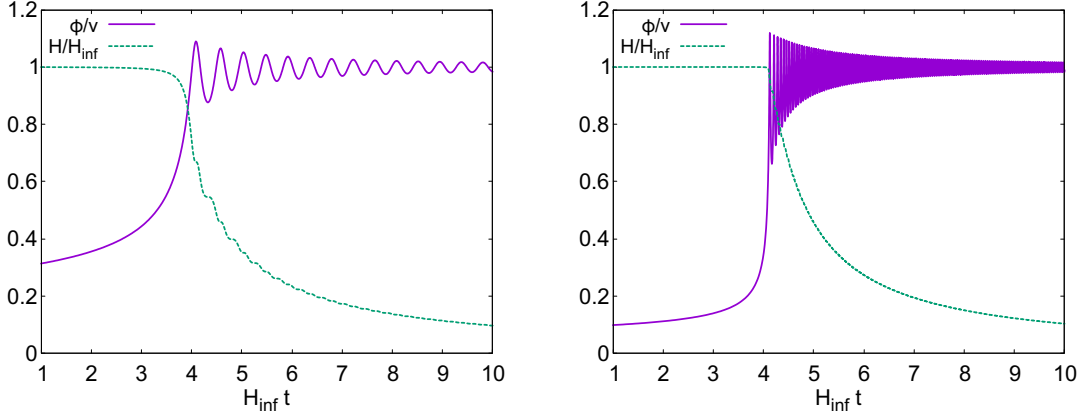


Figure 5: Time evolution of the homogeneous inflaton field ϕ/v (solid) and the Hubble parameter H/H_{inf} (dashed) in the new inflation model. We have taken $v/M_{\text{Pl}} = 1$ in the left panel and $v/M_{\text{Pl}} = 0.1$ in the right panel.

The inflaton mass around the minimum is

$$m_\phi = \frac{\sqrt{2}n\Lambda^2}{v} = \frac{\sqrt{6}nM_{\text{Pl}}}{v} H_e \quad \leftrightarrow \quad \frac{H_e}{m_\phi} = \frac{v}{\sqrt{6}nM_{\text{Pl}}}. \quad (47)$$

Therefore there is a large hierarchy between the inflaton mass and inflationary Hubble scale for smaller v , and hence f_2/f_1 also becomes large (see Fig. 2).

As an example, let us consider the case of $n = 4$. In this case, to reproduce the density perturbation $\mathcal{P}_\zeta = 2.2 \times 10^{-9}$, we obtain

$$\Lambda \simeq 9 \times 10^{14} \text{ GeV} \left(\frac{v}{M_{\text{Pl}}} \right) \left(\frac{60}{N} \right)^{\frac{3}{4}}. \quad (48)$$

The inflaton mass and inflationary Hubble scale are given by

$$m_\phi \simeq 2 \times 10^{12} \text{ GeV} \left(\frac{v}{M_{\text{Pl}}} \right) \left(\frac{60}{N} \right)^{\frac{3}{2}}, \quad H_e \simeq 2 \times 10^{11} \text{ GeV} \left(\frac{v}{M_{\text{Pl}}} \right)^2 \left(\frac{60}{N} \right)^{\frac{3}{2}}. \quad (49)$$

Fig. 5 shows the time evolution of the inflaton field for $v/M_{\text{Pl}} = 1$ (left panel) and $v/M_{\text{Pl}} = 0.1$ (right panel). It is seen that the oscillation time scale, m_ϕ^{-1} , which is much shorter than the Hubble scale H_e^{-1} , soon appears after inflation ends. Thus the transition from inflationary era to the inflaton oscillation era is close to instantaneous and a rough picture depicted in Fig. 2 is expected to apply.⁹

The result of numerical calculation for the GW spectrum are shown in Fig. 6. We have taken $v/M_{\text{Pl}} = 1$ (left panel) and $v/M_{\text{Pl}} = 0.1$ (right panel). We can see the f^{-2} and $f^{-1/2}$

⁹In reality, the inflaton fluctuation grows as the inflaton starts to oscillate and we should take account of the spatially inhomogeneous distributions [55, 56]. In this paper we do not go into detail of this aspect.

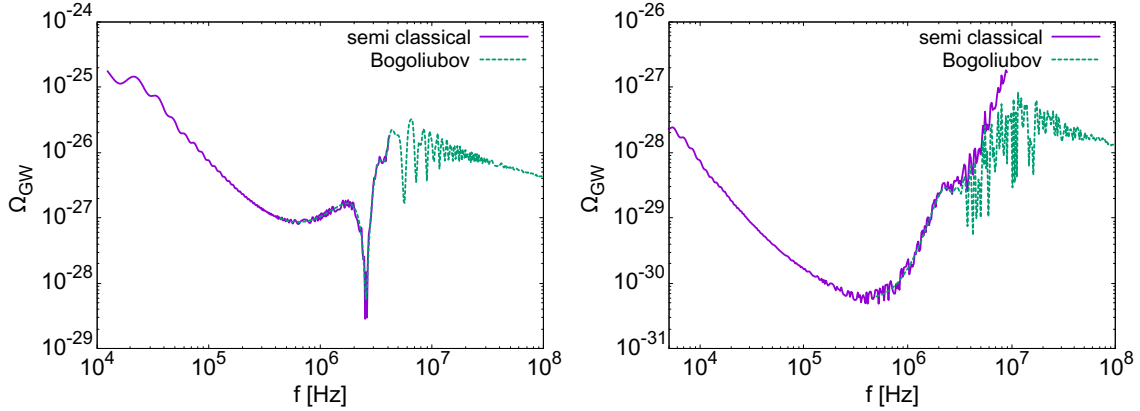


Figure 6: GW spectrum in new inflation model. We have taken $v/M_{\text{Pl}} = 1$ in the left panel and $v/M_{\text{Pl}} = 0.1$ in the right panel.

behavior in the low-frequency ($f < f_1$) and high-frequency ($f > f_2$) limit, respectively. They are perfectly consistent with the rough estimation in Sec. 2.3 with $w = 0$ and also a schematic picture shown in Fig. 2. Our numerical simulation revealed the structure in the intermediate frequency region $f_1 \lesssim f \lesssim f_2$. Although there are some nontrivial oscillatory behavior there, as an overall structure, the spectrum roughly monotonically increases from $\Omega_{\text{GW}}(f_1)$ to $\Omega_{\text{GW}}(f_2)$.

3.4 Attractor inflation

Finally let us consider the α -attractor T model [57–59]. This model utilizes the kinetic term like $\mathcal{L} \sim -f(\phi)(\partial\phi)^2/2$ with $f(\phi) \sim (1 - \phi^2/\Lambda^2)^{-2}$, which is divergent at $\phi = \Lambda$. After redefining the inflaton field so that it is canonically normalized (and rewrite the canonical inflaton as ϕ), the scalar potential typically looks like

$$V = \frac{\lambda}{n} \left[\Lambda \tanh \left(\frac{|\phi|}{\Lambda} \right) \right]^n, \quad (50)$$

where λ is a constant. The dimensionless power spectrum is given by

$$\mathcal{P}_\zeta = \frac{N^2 \lambda \Lambda^{n-2}}{3n\pi^2 M_{\text{Pl}}^2}. \quad (51)$$

The scalar spectral index and tensor-to-scalar ratio are given by

$$n_s = 1 - \frac{2}{N}, \quad r = \frac{2}{N^2} \left(\frac{\Lambda}{M_{\text{Pl}}} \right)^2. \quad (52)$$

For $n = 2$, the inflaton mass is identified as $m_\phi = \sqrt{\lambda}$ and it is determined to reproduced

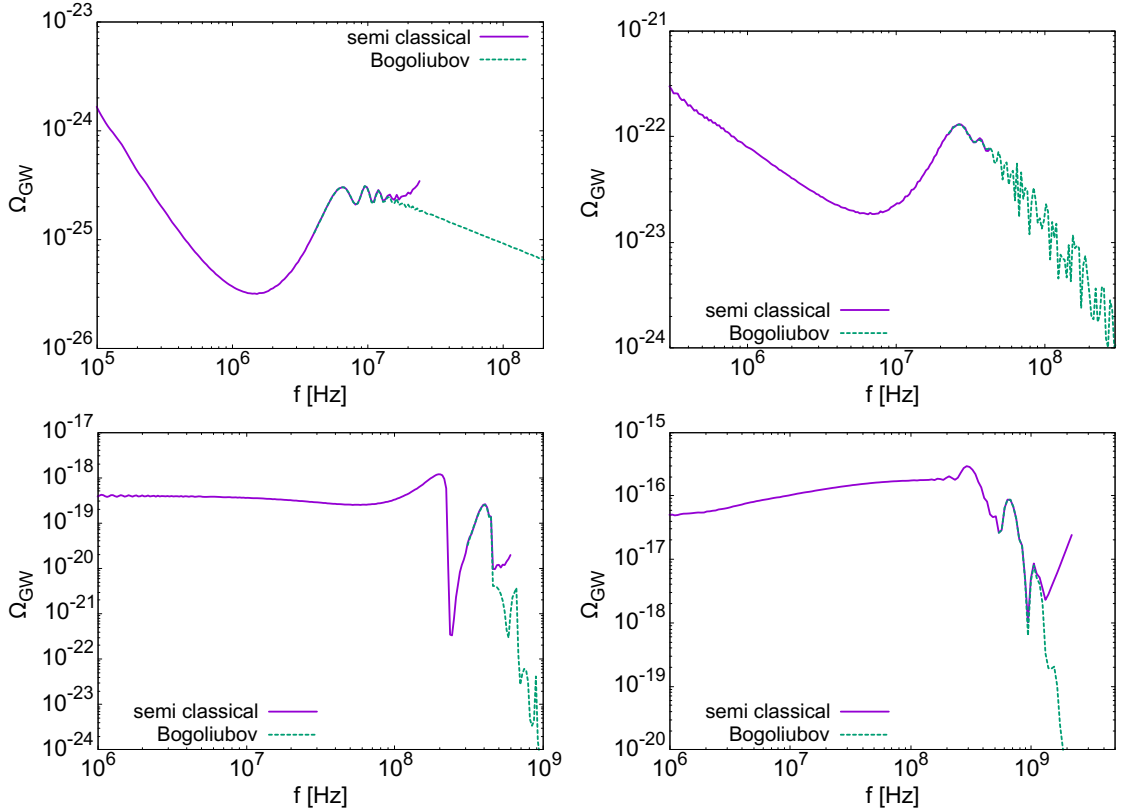


Figure 7: GW spectrum in the T-model with $n = 2$ (upper left), $n = 2.5$ (upper right), $n = 4$ (lower left) and $n = 6$ (lower right). We have taken $\Lambda/M_{\text{Pl}} = 0.5$.

the observed density perturbation. The inflaton mass and the Hubble scale are given by

$$m_\phi \simeq 1.4 \times 10^{13} \text{ GeV} \left(\frac{60}{N} \right), \quad \frac{H_e}{m_\phi} = \frac{\Lambda}{\sqrt{6} M_{\text{Pl}}}. \quad (53)$$

Therefore, for $\Lambda \ll M_{\text{Pl}}$ we have hierarchy $H_e \ll m_\phi$. For general n , the coupling constant λ is given by

$$\lambda M_{\text{Pl}}^{n-4} = \frac{3\pi^2 n \mathcal{P}_\zeta}{N^2} \left(\frac{M_{\text{Pl}}}{\Lambda} \right)^{n-2}, \quad (54)$$

and defining $m_\phi^2(t_e) = \lambda \Lambda^{n-2}$, we obtain

$$m_\phi(t_e) \simeq \frac{\sqrt{3\pi^2 n \mathcal{P}_\zeta}}{N} M_{\text{Pl}}, \quad \frac{H_e}{m_\phi(t_e)} \simeq \frac{\Lambda}{\sqrt{3n} M_{\text{Pl}}}. \quad (55)$$

The result of numerical calculation for the GW spectrum are shown in Fig. 7 for $n = 2$ (upper left), $n = 2.5$ (upper right), $n = 4$ (lower left) and $n = 6$ (lower right). We have

taken $\Lambda/M_{\text{Pl}} = 0.5$. The behavior for $n = 2$ is more or less similar to the previous cases like Starobinsky or new inflation models since we have $w = 0$: we can see both f^{-2} and $f^{-1/2}$ scaling at low- and high-frequency limit, respectively. Similarly, for $n = 2.5$, we have f^{-1} and f^{-2} scalings, which are also consistent with the estimate in Sec. 2.3. For $n = 4$, we effectively have $w = 1/3$ during the inflaton oscillation and hence we have flat GW spectrum for those experienced the superhorizon regime during inflation, as expected from analytic estimate Eq. (28). GWs with higher frequency never experience significant particle production from the inflaton oscillation because they never hits the condition $k = a(t)m_\phi(t)$ (see left panel of Fig. 3 with $w = 1/3$). Thus the spectrum rapidly decreases for $f \gg f_2$.

4 Conclusions and discussion

Inflation produces stochastic GW background with an extremely wide frequency range. Even very high frequency GWs which never exit the horizon are amplified through the post-inflationary dynamics of the inflaton. It is not very difficult to analytically estimate the resulting GW spectrum both in the low and high frequency limit, but there is an intermediate frequency region in which an analytic estimation is difficult. In particular, in a standard reheating model in which the inflaton oscillates with a quadratic potential, there is a gap in the GW spectrum between the low- and high-frequency regimes. This gap is represented by a ratio between the inflaton mass and Hubble scale (36) (see also Fig. 2), which is typically (much) larger than unity, and the spectrum that connects between two values is nontrivial. We have developed useful methods to precisely calculate the GW spectrum including such an intermediate frequency range, and performed numerical calculations for some concrete inflation models. We confirmed the analytic results for the low and high frequency limit, while we found a peculiar structure in the GW spectrum in the intermediate range. Such structures may contain detailed information about the inflaton potential and be useful for distinguishing the inflation model.

While such high frequency GW spectrum shows interesting features, it should be noticed that its abundance is too small to detect in near future. Moreover, it may be hidden by the other GW sources: for example, bremsstrahlung GWs emitted at the inflaton decay [60–64], a possible inflaton decay into the graviton pair [65–69], GWs from scattering of Standard Model particles [70–73], and GWs from large density fluctuations through preheating [74–80]. However, the frequency dependence of these sources are much different from the one we derived and it is possible that the GW spectrum derived in this paper gives dominant contribution in some frequency range and hence still valuable to give precise prediction of the primordial GW spectrum.

Acknowledgment

This work was supported by World Premier International Research Center Initiative (WPI), MEXT, Japan. This work was also supported by JSPS KAKENHI (Grant Number 24K07010

[KN]).

A Convention

Let us define the tensor perturbation h_{ij} as

$$ds^2 = -dt^2 + a^2(t)(\delta_{ij} + c_1 h_{ij}(t, \vec{x}))dx^i dx^j, \quad (56)$$

with a numerical factor c_1 , which is usually taken to be 1 or 2 depending on the literature. When the GW propagates along the z direction, it is further decomposed as

$$h_{ij} = c_2 \begin{pmatrix} h_+ & h_\times & 0 \\ h_\times & -h_+ & 0 \\ 0 & 0 & 0 \end{pmatrix}, \quad (57)$$

where c_2 is another numerical factor, which is usually taken to be 1 or $1/\sqrt{2}$ depending on the literature, corresponding to the convention of the polarization sum $e_{ij}^\lambda e_{ij}^{*\lambda'} = 2c_2^2 \delta_{\lambda\lambda'}$, when h_{ij} is expanded as Eq. (2). The Einstein-Hilbert action is expanded as

$$\mathcal{L} = \frac{M_{\text{Pl}}^2}{2} R = -\frac{c_1^2 M_{\text{Pl}}^2}{8} (\partial_\mu h_{\rho\sigma})^2 = -\frac{c_1^2 c_2^2 M_{\text{Pl}}^2}{4} \sum_{\lambda=+,\times} (\partial_\mu h_\lambda)^2, \quad (58)$$

in the transverse-traceless gauge $\partial_i h_{ij} = h_i^i = 0$ for the on-shell graviton. The canonical graviton is therefore

$$h_\lambda^{(\text{can})} \equiv \frac{c_1 c_2 M_{\text{Pl}}}{\sqrt{2}} h_\lambda. \quad (59)$$

With these definitions, the dimensionless tensor power spectrum in the de-Sitter universe in the superhorizon limit is

$$\Delta_{h^{(\text{can})}}^2 = c_3 \left(\frac{H_{\text{inf}}}{2\pi} \right)^2 \quad \rightarrow \quad \Delta_h^2 = \frac{c_3}{c_1^2 c_2^2 2\pi^2} \left(\frac{H_{\text{inf}}}{M_{\text{Pl}}} \right)^2, \quad (60)$$

where c_3 is a numerical factor. If one defines $\Delta_{h^{(\text{can})}}^2$ as a sum of two polarizations, we should choose $c_3 = 2$. If one defines $\Delta_{h^{(\text{can})}}^2$ for each polarization, we may take $c_3 = 1$. The dimensionless power spectrum of the curvature perturbation is given by

$$\Delta_\zeta^2 = \left(\frac{H_{\text{inf}}}{\dot{\phi}} \frac{H_{\text{inf}}}{2\pi} \right)^2 = \frac{1}{2\epsilon M_{\text{Pl}}^2} \left(\frac{H_{\text{inf}}}{2\pi} \right)^2. \quad (61)$$

where ϵ is a slow-roll parameter. The tensor-to-scalar ratio is then defined by

$$r \equiv c_4 \frac{\Delta_h^2}{\Delta_\zeta^2} = \frac{c_3 c_4}{c_1^2 c_2^2} \times 4\epsilon, \quad (62)$$

where c_4 is another numerical factor. In this paper we take $c_1 = 1, c_2 = 1/\sqrt{2}, c_3 = 2, c_4 = 1$,¹⁰ which yields $r = 16\epsilon$.

¹⁰This convention is the same as e.g. Ref. [81].

References

- [1] A. A. Starobinsky, “A New Type of Isotropic Cosmological Models Without Singularity,” *Phys. Lett. B* **91** (1980) 99–102.
- [2] A. H. Guth, “The Inflationary Universe: A Possible Solution to the Horizon and Flatness Problems,” *Phys. Rev. D* **23** (1981) 347–356.
- [3] K. Sato, “First-order phase transition of a vacuum and the expansion of the Universe,” *Mon. Not. Roy. Astron. Soc.* **195** no. 3, (1981) 467–479.
- [4] D. Kazanas, “Dynamics of the Universe and Spontaneous Symmetry Breaking,” *Astrophys. J. Lett.* **241** (1980) L59–L63.
- [5] A. D. Linde, “A New Inflationary Universe Scenario: A Possible Solution of the Horizon, Flatness, Homogeneity, Isotropy and Primordial Monopole Problems,” *Phys. Lett. B* **108** (1982) 389–393.
- [6] A. Albrecht and P. J. Steinhardt, “Cosmology for Grand Unified Theories with Radiatively Induced Symmetry Breaking,” *Phys. Rev. Lett.* **48** (1982) 1220–1223.
- [7] A. A. Starobinsky, “Spectrum of relict gravitational radiation and the early state of the universe,” *JETP Lett.* **30** (1979) 682–685.
- [8] B. Allen, “The Stochastic Gravity Wave Background in Inflationary Universe Models,” *Phys. Rev. D* **37** (1988) 2078.
- [9] M. S. Turner and F. Wilczek, “Relic gravitational waves and extended inflation,” *Phys. Rev. Lett.* **65** (1990) 3080–3083.
- [10] M. S. Turner, M. J. White, and J. E. Lidsey, “Tensor perturbations in inflationary models as a probe of cosmology,” *Phys. Rev. D* **48** (1993) 4613–4622, [arXiv:astro-ph/9306029](https://arxiv.org/abs/astro-ph/9306029).
- [11] M. S. Turner, “Detectability of inflation produced gravitational waves,” *Phys. Rev. D* **55** (1997) R435–R439, [arXiv:astro-ph/9607066](https://arxiv.org/abs/astro-ph/9607066).
- [12] T. L. Smith, M. Kamionkowski, and A. Cooray, “Direct detection of the inflationary gravitational wave background,” *Phys. Rev. D* **73** (2006) 023504, [arXiv:astro-ph/0506422](https://arxiv.org/abs/astro-ph/0506422).
- [13] L. A. Boyle and P. J. Steinhardt, “Probing the early universe with inflationary gravitational waves,” *Phys. Rev. D* **77** (2008) 063504, [arXiv:astro-ph/0512014](https://arxiv.org/abs/astro-ph/0512014).
- [14] N. Seto and J. Yokoyama, “Probing the equation of state of the early universe with a space laser interferometer,” *J. Phys. Soc. Jap.* **72** (2003) 3082–3086, [arXiv:gr-qc/0305096](https://arxiv.org/abs/gr-qc/0305096).

- [15] H. Tashiro, T. Chiba, and M. Sasaki, “Reheating after quintessential inflation and gravitational waves,” *Class. Quant. Grav.* **21** (2004) 1761–1772, [arXiv:gr-qc/0307068](https://arxiv.org/abs/gr-qc/0307068).
- [16] K. Nakayama, S. Saito, Y. Suwa, and J. Yokoyama, “Space laser interferometers can determine the thermal history of the early Universe,” *Phys. Rev. D* **77** (2008) 124001, [arXiv:0802.2452 \[hep-ph\]](https://arxiv.org/abs/0802.2452).
- [17] K. Nakayama, S. Saito, Y. Suwa, and J. Yokoyama, “Probing reheating temperature of the universe with gravitational wave background,” *JCAP* **06** (2008) 020, [arXiv:0804.1827 \[astro-ph\]](https://arxiv.org/abs/0804.1827).
- [18] S. Kuroyanagi, T. Chiba, and N. Sugiyama, “Precision calculations of the gravitational wave background spectrum from inflation,” *Phys. Rev. D* **79** (2009) 103501, [arXiv:0804.3249 \[astro-ph\]](https://arxiv.org/abs/0804.3249).
- [19] S. Mukohyama, K. Nakayama, F. Takahashi, and S. Yokoyama, “Phenomenological Aspects of Horava-Lifshitz Cosmology,” *Phys. Lett. B* **679** (2009) 6–9, [arXiv:0905.0055 \[hep-th\]](https://arxiv.org/abs/0905.0055).
- [20] K. Nakayama and J. Yokoyama, “Gravitational Wave Background and Non-Gaussianity as a Probe of the Curvaton Scenario,” *JCAP* **01** (2010) 010, [arXiv:0910.0715 \[astro-ph.CO\]](https://arxiv.org/abs/0910.0715).
- [21] R. Durrer and J. Hasenkamp, “Testing Superstring Theories with Gravitational Waves,” *Phys. Rev. D* **84** (2011) 064027, [arXiv:1105.5283 \[gr-qc\]](https://arxiv.org/abs/1105.5283).
- [22] R. Jinno, T. Moroi, and K. Nakayama, “Imprints of Cosmic Phase Transition in Inflationary Gravitational Waves,” *Phys. Lett. B* **713** (2012) 129–132, [arXiv:1112.0084 \[hep-ph\]](https://arxiv.org/abs/1112.0084).
- [23] S. Kuroyanagi, K. Nakayama, and S. Saito, “Prospects for determination of thermal history after inflation with future gravitational wave detectors,” *Phys. Rev. D* **84** (2011) 123513, [arXiv:1110.4169 \[astro-ph.CO\]](https://arxiv.org/abs/1110.4169).
- [24] R. Jinno, T. Moroi, and K. Nakayama, “Probing dark radiation with inflationary gravitational waves,” *Phys. Rev. D* **86** (2012) 123502, [arXiv:1208.0184 \[astro-ph.CO\]](https://arxiv.org/abs/1208.0184).
- [25] R. Jinno, T. Moroi, and K. Nakayama, “Inflationary Gravitational Waves and the Evolution of the Early Universe,” *JCAP* **01** (2014) 040, [arXiv:1307.3010 \[hep-ph\]](https://arxiv.org/abs/1307.3010).
- [26] R. Jinno, T. Moroi, and T. Takahashi, “Studying Inflation with Future Space-Based Gravitational Wave Detectors,” *JCAP* **12** (2014) 006, [arXiv:1406.1666 \[astro-ph.CO\]](https://arxiv.org/abs/1406.1666).

- [27] S. Kuroyanagi, K. Nakayama, and J. Yokoyama, “Prospects of determination of reheating temperature after inflation by DECIGO,” *PTEP* **2015** no. 1, (2015) 013E02, [arXiv:1410.6618 \[astro-ph.CO\]](https://arxiv.org/abs/1410.6618).
- [28] K. Minami, K. Mukaida, and K. Nakayama, “Reheating with Thermal Dissipation and Primordial Gravitational Waves,” [arXiv:2510.02481 \[astro-ph.CO\]](https://arxiv.org/abs/2510.02481).
- [29] Y. Ema, R. Jinno, K. Mukaida, and K. Nakayama, “Gravitational Effects on Inflaton Decay,” *JCAP* **05** (2015) 038, [arXiv:1502.02475 \[hep-ph\]](https://arxiv.org/abs/1502.02475).
- [30] Y. Ema, R. Jinno, K. Mukaida, and K. Nakayama, “Gravitational particle production in oscillating backgrounds and its cosmological implications,” *Phys. Rev. D* **94** no. 6, (2016) 063517, [arXiv:1604.08898 \[hep-ph\]](https://arxiv.org/abs/1604.08898).
- [31] Y. Ema, R. Jinno, and K. Nakayama, “High-frequency Graviton from Inflaton Oscillation,” *JCAP* **09** (2020) 015, [arXiv:2006.09972 \[astro-ph.CO\]](https://arxiv.org/abs/2006.09972).
- [32] A. D. Dolgov and D. P. Kirilova, “ON PARTICLE CREATION BY A TIME DEPENDENT SCALAR FIELD,” *Sov. J. Nucl. Phys.* **51** (1990) 172–177.
- [33] J. H. Traschen and R. H. Brandenberger, “Particle Production During Out-of-equilibrium Phase Transitions,” *Phys. Rev. D* **42** (1990) 2491–2504.
- [34] Y. Shtanov, J. H. Traschen, and R. H. Brandenberger, “Universe reheating after inflation,” *Phys. Rev. D* **51** (1995) 5438–5455, [arXiv:hep-ph/9407247](https://arxiv.org/abs/hep-ph/9407247).
- [35] L. Kofman, A. D. Linde, and A. A. Starobinsky, “Reheating after inflation,” *Phys. Rev. Lett.* **73** (1994) 3195–3198, [arXiv:hep-th/9405187](https://arxiv.org/abs/hep-th/9405187).
- [36] L. Kofman, A. D. Linde, and A. A. Starobinsky, “Towards the theory of reheating after inflation,” *Phys. Rev. D* **56** (1997) 3258–3295, [arXiv:hep-ph/9704452](https://arxiv.org/abs/hep-ph/9704452).
- [37] G. Choi, W. Ke, and K. A. Olive, “Minimal production of prompt gravitational waves during reheating,” *Phys. Rev. D* **109** no. 8, (2024) 083516, [arXiv:2402.04310 \[hep-ph\]](https://arxiv.org/abs/2402.04310).
- [38] Y. Xu, “Ultra-high frequency gravitational waves from scattering, Bremsstrahlung and decay during reheating,” *JHEP* **10** (2024) 174, [arXiv:2407.03256 \[hep-ph\]](https://arxiv.org/abs/2407.03256).
- [39] N. Bernal, Q.-f. Wu, X.-J. Xu, and Y. Xu, “Pre-thermalized gravitational waves,” *JHEP* **08** (2025) 125, [arXiv:2503.10756 \[hep-ph\]](https://arxiv.org/abs/2503.10756).
- [40] K. D. Lozanov and M. A. Amin, “Self-resonance after inflation: oscillons, transients and radiation domination,” *Phys. Rev. D* **97** no. 2, (2018) 023533, [arXiv:1710.06851 \[astro-ph.CO\]](https://arxiv.org/abs/1710.06851).

- [41] M. A. G. Garcia, M. Gross, Y. Mambrini, K. A. Olive, M. Pierre, and J.-H. Yoon, “Effects of fragmentation on post-inflationary reheating,” *JCAP* **12** (2023) 028, [arXiv:2308.16231 \[hep-ph\]](https://arxiv.org/abs/2308.16231).
- [42] C. Eröncel, Y. Gouttenoire, R. Sato, G. Servant, and P. Simakachorn, “Universal Bound on the Duration of a Kination Era,” *Phys. Rev. Lett.* **135** no. 10, (2025) 101002, [arXiv:2501.17226 \[hep-ph\]](https://arxiv.org/abs/2501.17226).
- [43] **Planck** Collaboration, N. Aghanim *et al.*, “Planck 2018 results. VI. Cosmological parameters,” *Astron. Astrophys.* **641** (2020) A6, [arXiv:1807.06209 \[astro-ph.CO\]](https://arxiv.org/abs/1807.06209). [Erratum: *Astron. Astrophys.* 652, C4 (2021)].
- [44] A. D. Linde, “Chaotic Inflation,” *Phys. Lett. B* **129** (1983) 177–181.
- [45] D. H. Lyth and A. R. Liddle, *The Primordial Density Perturbation*. 6, 2009.
- [46] D. S. Gorbunov and A. G. Panin, “Scalaron the mighty: producing dark matter and baryon asymmetry at reheating,” *Phys. Lett. B* **700** (2011) 157–162, [arXiv:1009.2448 \[hep-ph\]](https://arxiv.org/abs/1009.2448).
- [47] Q. Li, T. Moroi, K. Nakayama, and W. Yin, “Hidden dark matter from Starobinsky inflation,” *JHEP* **09** (2021) 179, [arXiv:2105.13358 \[hep-ph\]](https://arxiv.org/abs/2105.13358).
- [48] K. Kumekawa, T. Moroi, and T. Yanagida, “Flat potential for inflaton with a discrete R invariance in supergravity,” *Prog. Theor. Phys.* **92** (1994) 437–448, [arXiv:hep-ph/9405337](https://arxiv.org/abs/hep-ph/9405337).
- [49] K. I. Izawa and T. Yanagida, “Natural new inflation in broken supergravity,” *Phys. Lett. B* **393** (1997) 331–336, [arXiv:hep-ph/9608359](https://arxiv.org/abs/hep-ph/9608359).
- [50] T. Asaka, K. Hamaguchi, M. Kawasaki, and T. Yanagida, “Leptogenesis in inflationary universe,” *Phys. Rev. D* **61** (2000) 083512, [arXiv:hep-ph/9907559](https://arxiv.org/abs/hep-ph/9907559).
- [51] V. N. Senoguz and Q. Shafi, “New inflation, preinflation, and leptogenesis,” *Phys. Lett. B* **596** (2004) 8–15, [arXiv:hep-ph/0403294](https://arxiv.org/abs/hep-ph/0403294).
- [52] K. Kohri, C.-M. Lin, and D. H. Lyth, “More hilltop inflation models,” *JCAP* **12** (2007) 004, [arXiv:0707.3826 \[hep-ph\]](https://arxiv.org/abs/0707.3826).
- [53] K. Nakayama and F. Takahashi, “PeV-scale Supersymmetry from New Inflation,” *JCAP* **05** (2012) 035, [arXiv:1203.0323 \[hep-ph\]](https://arxiv.org/abs/1203.0323).
- [54] Y. Ema, K. Mukaida, and K. Nakayama, “Electroweak Vacuum Metastability and Low-scale Inflation,” *JCAP* **12** (2017) 030, [arXiv:1706.08920 \[hep-ph\]](https://arxiv.org/abs/1706.08920).
- [55] P. Brax, J.-F. Dufaux, and S. Mariadassou, “Preheating after Small-Field Inflation,” *Phys. Rev. D* **83** (2011) 103510, [arXiv:1012.4656 \[hep-th\]](https://arxiv.org/abs/1012.4656).

[56] S. Antusch, F. Cefala, D. Nolde, and S. Orani, “Parametric resonance after hilltop inflation caused by an inhomogeneous inflaton field,” *JCAP* **02** (2016) 044, [arXiv:1510.04856 \[hep-ph\]](https://arxiv.org/abs/1510.04856).

[57] R. Kallosh and A. Linde, “Universality Class in Conformal Inflation,” *JCAP* **07** (2013) 002, [arXiv:1306.5220 \[hep-th\]](https://arxiv.org/abs/1306.5220).

[58] R. Kallosh, A. Linde, and D. Roest, “Superconformal Inflationary α -Attractors,” *JHEP* **11** (2013) 198, [arXiv:1311.0472 \[hep-th\]](https://arxiv.org/abs/1311.0472).

[59] M. Galante, R. Kallosh, A. Linde, and D. Roest, “Unity of Cosmological Inflation Attractors,” *Phys. Rev. Lett.* **114** no. 14, (2015) 141302, [arXiv:1412.3797 \[hep-th\]](https://arxiv.org/abs/1412.3797).

[60] K. Nakayama and Y. Tang, “Stochastic Gravitational Waves from Particle Origin,” *Phys. Lett. B* **788** (2019) 341–346, [arXiv:1810.04975 \[hep-ph\]](https://arxiv.org/abs/1810.04975). [Erratum: *Phys.Lett.B* 839, 137787 (2023)].

[61] B. Barman, N. Bernal, Y. Xu, and Ó. Zapata, “Gravitational wave from graviton Bremsstrahlung during reheating,” *JCAP* **05** (2023) 019, [arXiv:2301.11345 \[hep-ph\]](https://arxiv.org/abs/2301.11345).

[62] B. Barman, N. Bernal, Y. Xu, and Ó. Zapata, “Bremsstrahlung-induced gravitational waves in monomial potentials during reheating,” *Phys. Rev. D* **108** no. 8, (2023) 083524, [arXiv:2305.16388 \[hep-ph\]](https://arxiv.org/abs/2305.16388).

[63] W. Hu, K. Nakayama, V. Takhistov, and Y. Tang, “Gravitational wave probe of Planck-scale physics after inflation,” *Phys. Lett. B* **856** (2024) 138958, [arXiv:2403.13882 \[hep-ph\]](https://arxiv.org/abs/2403.13882).

[64] W.-Y. Hu, K. Nakayama, V. Takhistov, and Y. Tang, “Dual gravitational wave signatures of instant preheating,” *JCAP* **01** (2025) 029, [arXiv:2409.06483 \[astro-ph.CO\]](https://arxiv.org/abs/2409.06483).

[65] Y. Ema, K. Mukaida, and K. Nakayama, “Scalar field couplings to quadratic curvature and decay into gravitons,” *JHEP* **05** (2022) 087, [arXiv:2112.12774 \[hep-ph\]](https://arxiv.org/abs/2112.12774).

[66] K. Mudrunka and K. Nakayama, “Probing Gauss-Bonnet-corrected inflation with gravitational waves,” *JCAP* **05** (2024) 069, [arXiv:2312.15766 \[astro-ph.CO\]](https://arxiv.org/abs/2312.15766).

[67] A. Tokareva, “Gravitational waves from inflaton decay and bremsstrahlung,” *Phys. Lett. B* **853** (2024) 138695, [arXiv:2312.16691 \[hep-ph\]](https://arxiv.org/abs/2312.16691).

[68] A. Strumia and G. Landini, “Optical gravitational waves as signals of gravitationally-decaying particles,” *JHEP* **04** (2025) 068, [arXiv:2501.09794 \[hep-ph\]](https://arxiv.org/abs/2501.09794).

- [69] K. Nakayama, F. Takahashi, and J. Wada, “Gravitational Decays of Secluded Scalars and Graviton Dark Radiation,” [arXiv:2512.03662](https://arxiv.org/abs/2512.03662) [hep-ph].
- [70] J. Ghiglieri and M. Laine, “Gravitational wave background from Standard Model physics: Qualitative features,” *JCAP* **07** (2015) 022, [arXiv:1504.02569](https://arxiv.org/abs/1504.02569) [hep-ph].
- [71] J. Ghiglieri, G. Jackson, M. Laine, and Y. Zhu, “Gravitational wave background from Standard Model physics: Complete leading order,” *JHEP* **07** (2020) 092, [arXiv:2004.11392](https://arxiv.org/abs/2004.11392) [hep-ph].
- [72] A. Ringwald, J. Schütte-Engel, and C. Tamarit, “Gravitational Waves as a Big Bang Thermometer,” *JCAP* **03** (2021) 054, [arXiv:2011.04731](https://arxiv.org/abs/2011.04731) [hep-ph].
- [73] J. Ghiglieri, J. Schütte-Engel, and E. Speranza, “Freezing-in gravitational waves,” *Phys. Rev. D* **109** no. 2, (2024) 023538, [arXiv:2211.16513](https://arxiv.org/abs/2211.16513) [hep-ph].
- [74] S. Y. Khlebnikov and I. I. Tkachev, “Relic gravitational waves produced after preheating,” *Phys. Rev. D* **56** (1997) 653–660, [arXiv:hep-ph/9701423](https://arxiv.org/abs/hep-ph/9701423).
- [75] R. Easter, J. T. Giblin, Jr., and E. A. Lim, “Gravitational Wave Production At The End Of Inflation,” *Phys. Rev. Lett.* **99** (2007) 221301, [arXiv:astro-ph/0612294](https://arxiv.org/abs/astro-ph/0612294).
- [76] R. Easter and E. A. Lim, “Stochastic gravitational wave production after inflation,” *JCAP* **04** (2006) 010, [arXiv:astro-ph/0601617](https://arxiv.org/abs/astro-ph/0601617).
- [77] J. Garcia-Bellido and D. G. Figueroa, “A stochastic background of gravitational waves from hybrid preheating,” *Phys. Rev. Lett.* **98** (2007) 061302, [arXiv:astro-ph/0701014](https://arxiv.org/abs/astro-ph/0701014).
- [78] J. Garcia-Bellido, D. G. Figueroa, and A. Sastre, “A Gravitational Wave Background from Reheating after Hybrid Inflation,” *Phys. Rev. D* **77** (2008) 043517, [arXiv:0707.0839](https://arxiv.org/abs/0707.0839) [hep-ph].
- [79] J. F. Dufaux, A. Bergman, G. N. Felder, L. Kofman, and J.-P. Uzan, “Theory and Numerics of Gravitational Waves from Preheating after Inflation,” *Phys. Rev. D* **76** (2007) 123517, [arXiv:0707.0875](https://arxiv.org/abs/0707.0875) [astro-ph].
- [80] J.-F. Dufaux, G. Felder, L. Kofman, and O. Navros, “Gravity Waves from Tachyonic Preheating after Hybrid Inflation,” *JCAP* **03** (2009) 001, [arXiv:0812.2917](https://arxiv.org/abs/0812.2917) [astro-ph].
- [81] D. Baumann, *Cosmology*. Cambridge University Press, 7, 2022.